

Spin multiplicity and charge state of a silicon vacancy (T_{V2a}) in 4H-SiC determined by pulsed ENDOR

N. Mizuochi,^{1,2} S. Yamasaki,^{2,3} H. Takizawa,⁴ N. Morishita,⁴ T. Ohshima,⁴ H. Itoh,⁴ T. Umeda,¹ and J. Isoya^{1,2}

¹Graduate School of Library, Information and Media Studies, University of Tsukuba, 1-2 Kasuga, Tsukuba-City, Ibaraki 305-8550, Japan

²Diamond Research Center, National Institute of Advanced Industrial Science and Technology (AIST), Tsukuba Central 2, 1-1-1 Umezono, Tsukuba-City, Ibaraki 305-8568, Japan

³Institute of Applied Physics, University of Tsukuba, 1-1-1 Tennodai, Tsukuba-City 305-8577, Japan

⁴Japan Atomic Energy Research Institute, 1233 Watanuki, Takasaki-City, Gunma 370-1292, Japan

(Received 15 August 2005; revised manuscript received 7 October 2005; published 28 December 2005)

In this paper, we unambiguously re-determine the spin multiplicity of T_{V2a} by pulsed electron nucleus double resonance technique. The T_{V2a} center is one of the most commonly observed defects in 4H-SiC, and its origin was identified as one belonging to a class of negatively charged silicon vacancy by means of continuous-wave electron paramagnetic resonance (EPR) and the two-dimensional nutation method of pulsed EPR technique. However, a model with the spin multiplicity of triplet ($S=1$) and the neutral charge state has recently been suggested. Our result clearly shows that T_{V2a} is a quartet spin ($S=3/2$) state and thus should be single-negatively charged (-1).

DOI: [10.1103/PhysRevB.72.235208](https://doi.org/10.1103/PhysRevB.72.235208)

PACS number(s): 61.72.Ji, 76.30.Mi

I. INTRODUCTION

In SiC, there are two types of fundamental lattice vacancies: the silicon vacancy and the carbon vacancy. Both of these strongly affect the electrical properties of this material. They are observed by electron paramagnetic resonance (EPR) or optically detected magnetic resonance (ODMR).¹ Using EPR or ODMR, these two types can be simply distinguished according to the hyperfine (HF) interactions due to the four nearest-neighbor (NN) atoms of a vacancy. For the carbon vacancy, the NN atoms are Si, so we can observe the NN ^{29}Si (nuclear spin $I=1/2$, natural abundance=4.7%) HF interactions. On the other hand, the NN ^{13}C ($I=1/2$, natural abundance=1.1%) HF interactions can be observed for the silicon vacancy. Among a number of EPR centers reported so far, those labeled $V_{\text{Si}}^-(\text{I,II})$ and T_{V2a} in 4H-SiC or 6H-SiC were found to generate the NN ^{13}C HF interactions.²⁻⁹ These three centers have been identified as a silicon vacancy distorted along the c axis ([0001]) with a C_{3v} symmetry.^{6,9-12} The g values of $V_{\text{Si}}^-(\text{I})$ and $V_{\text{Si}}^-(\text{II})$ cannot be distinguished in the X band. Therefore they were originally assigned as a single center and labeled as V_{Si}^- .¹³ From detailed angular analyses of the NN ^{13}C HF interactions with respect to crystal's rotation, they could be distinguished, and $V_{\text{Si}}^-(\text{I})$ and $V_{\text{Si}}^-(\text{II})$ were assigned as the silicon vacancies at the hexagonal and the quasicubic sites, respectively.⁹ $V_{\text{Si}}^-(\text{I,II})$ are very close to T_d symmetric geometry, while T_{V2a} is relatively distorted, resulting in the different EPR spectra.^{6,10-12} $V_{\text{Si}}^-(\text{I,II})$ do not exhibit zero-field splittings (ZFS) in the conventional X-band EPR, indicating that the deviation from T_d symmetric geometry is very small. On the other hand, T_{V2a} exhibits ZFS ($|D|=35.1$ MHz). The distortion of T_{V2a} , which is manifested in the ZFS, is likely to be caused by a perturbation of the crystal field, presumably by the presence of an accompanying impurity or defect located at some distance along the c axis ([0001]).⁶ As for the HF parameters of NN

carbon atoms, the difference between T_{V2a} and $V_{\text{Si}}^-(\text{I,II})$ is very small. These also indicate that the distortion of T_{V2a} is slightly larger than that of $V_{\text{Si}}^-(\text{I,II})$. Their HF parameters almost correspond to the theoretical values of the negatively charged vacancy in 4H-SiC.¹⁴ In addition, $V_{\text{Si}}^-(\text{I,II})$ and T_{V2a} are different in terms of thermal stability: $V_{\text{Si}}^-(\text{I,II})$ were annealed below 900 °C,^{4,15,16} but T_{V2a} remained up to higher temperatures.^{17,18} In particular, T_{V2a} was observed not only in irradiated SiC, but also in as-grown high-purity semi-insulating (HPSI) 4H-SiC,⁸ which is an important base material for wide-band-gap electronics.¹⁸ Therefore a Si vacancy labeled T_{V2a} is recognized as a possible candidate for the carrier-compensation center in this material and is thus a very important defect.

The EPR spectrum of T_{V2a} exhibits ZFS,^{2,3,5} indicating that T_{V2a} is a high spin state ($S>1/2$). Initially, the spin multiplicity of T_{V2a} was assigned to triplet ($S=1$), and T_{V2a} was thus regarded as a neutral Si vacancy.⁵ Later, from the two-dimensional (2D) nutation method of pulsed EPR technique, the spin multiplicity was clearly determined to be quartet ($S=3/2$). Accordingly, the charge state was reassigned to be a single-negatively charged state (-1). After this reassignment, however, the spin-1 ($S=1$) models were reported again based on a pulsed EPR study⁷ and a continuous-wave (cw) EPR study.⁸ Thus the spin multiplicity or the charge state of T_{V2a} is currently controversial. In contrast with T_{V2a} , quartet ($S=3/2$) and negative charge (-1) have been concluded for $V_{\text{Si}}^-(\text{I,II})$.¹³

It is important to determine the spin multiplicity of T_{V2a} for several reasons. One reason is that the charge state strongly influences the thermal stability of Si vacancies. First-principles calculations predicted that negatively charged Si vacancies could be stable in HPSI and n -type SiC, while other charge states of the silicon vacancy should not be stable because of their high formation energies. This naturally explains why Si vacancies are absent in p -type

materials.¹⁹ The spin-1 model for T_{V2a} , however, calls the above idea into question. Furthermore, there is the other question of why $V_{Si}^-(I,II)$ and T_{V2a} are simultaneously observed in thermal equilibrium (in dark).^{4,6,7} For the coexistence of the -1 and 0 charge states, the Fermi level should be very close to the ionization level of $(-/0)$ which was calculated to be located at 1.2 – 1.3 eV (Ref. 20) or 0.7 – 0.8 eV (Ref. 19) above the valence-band maximum. On the contrary, the equilibrium coexistence was observed in a variety of sample conditions such as different dopant concentrations and different radiation conditions.^{4,6,7} Furthermore, so far, except for the suggestion of the triplet state ($S=1$) on T_{V2a} , the electronic states of single vacancies which have a high spin ground state ($S>1/2$) in semiconductors are limited to the orbitally nondegenerate 4A_2 state ($S=3/2$), which is not subject to Jahn-Teller distortion. They are a single-negatively charged Si vacancy in $3C$ -, $4H$ -, $6H$ -SiC,^{9,13,21} a single-negatively charged vacancy in diamond,²² and a neutral Ga vacancy in GaP.^{23,24} The interactions between electrons such as the exchange interaction and the electron repulsion^{6,20} affect the determination of the ground state. For its elucidation, the experimental determination of the spin multiplicity of the ground state is important. Thus the spin multiplicity and charge state are related to significant issues that we have to answer.

In spin multiplicity determination, electron nucleus double resonance (ENDOR) spectroscopy can give crucial information. Treating the first order, the energy levels and the ENDOR frequencies for a spin system incorporating S and I are given by^{22,25}

$$E_{M_S, M_I} = M_S g_e \mu_e B + (M_S A_{\text{eff}} - g_n \mu_n B) M_I \quad (1)$$

and

$$\nu = (1/h) |M_S A_{\text{eff}} - g_n \mu_n B|, \quad (2)$$

respectively, where M_S and M_I are the magnetic quantum numbers ($|M_S| \leq 2S+1$, $|M_I| \leq 2I+1$) of electron spin and nuclear spin, respectively, $g_e \mu_e B$ is the electron Zeeman splitting, B is the applied magnetic field, A_{eff} is the HF splittings, and $g_n \mu_n B/h$ is the frequency of nuclear Zeeman splitting. Obviously, the ENDOR frequencies should be completely different depending on whether M_S values are -1 , 0 , $+1$ ($S=1$) or $-3/2$, $-1/2$, $+1/2$, $+3/2$ ($S=3/2$). In fact, the spin multiplicity of quartet ($S=3/2$) for V_{Si}^- has been unambiguously determined in this way.¹³ In this paper, we also demonstrate such a determination for T_{V2a} using a high-resolution pulsed-ENDOR spectrometer.

II. EXPERIMENT

The sample used in our experiments was single-crystalline n -type $4H$ -SiC (Nippon Steel: nitrogen dopant) with the carrier concentration of approximately $1 \times 10^{17}/\text{cm}^3$. A sample 1.5 mm thick was cut to a size (3×15 mm) appropriate for our EPR measurements in the X band. The crystal was irradiated by 3 -MeV electrons with the total fluence of $4 \times 10^{18} e/\text{cm}^2$. The sample was placed on a water-cooled holder to avoid beam heating and was kept below 330 K during the electron irradiation.

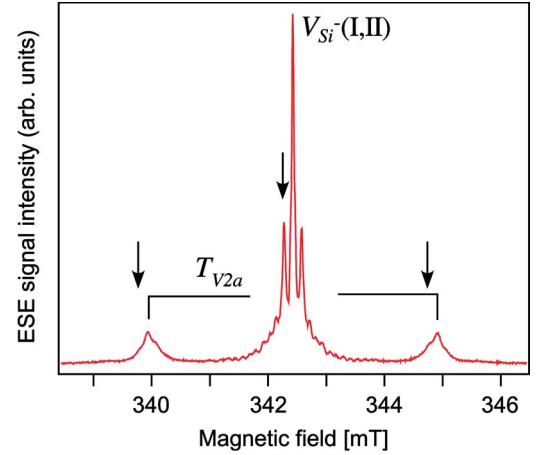


FIG. 1. (Color online) ESE spectrum of the electron-irradiated n -type $4H$ -SiC at room temperature taken with the magnetic field along the c axis ($[0001]$ axis). The microwave frequency was $\nu = 9.599$ GHz. The arrows indicate the magnetic field positions where the ENDOR spectra were measured.

Electron spin-echo (ESE) detected EPR and pulsed ENDOR experiments were carried out at room temperature in a dark condition on a Bruker ELEXXSYS X-band spectrometer. ESE experiment was performed using a two-pulse sequence (p_1 - τ - p_2) with the duration of microwave pulses p_1 and p_2 of 20 ns each and delay times τ of 1.2 μ s. Pulsed ENDOR experiments were performed using a three-pulse sequence (p_1 - τ - p_2 - T - p_3) with microwave pulses p_1 , p_2 , and p_3 20 ns wide and delay times τ and T of 800 ns and 16.2 μ s, respectively. During the time T an intense radiofrequency pulse 10 μ s wide was applied to the sample. Spectra were obtained by monitoring the echo while scanning the radiofrequency. In both experiments, the delay of 1 ms was used for repeating the pulse sequence in accumulation.

III. RESULTS AND DISCUSSION

The electron spin-echo (ESE) spectrum of the electron-irradiated $4H$ -SiC when the magnetic field was parallel to the c axis ($B \parallel c$) is shown in Fig. 1. In the central part of the spectrum, the negatively charged silicon vacancy [$V_{Si}^-(I,II)$, $g=2.0028$] is observed. On both sides of $V_{Si}^-(I,II)$,⁹ there are EPR signals labeled T_{V2a} . We measured the ENDOR spectra of them and confirmed their spin multiplicities. In the previous study, a T_{V2b} signal was also observed in the continuous-wave EPR spectrum of the same sample as the present study.⁶ The absence of it in Fig. 1 is due to the difference of the spin-relaxation times which affects the ESE signal intensity. First of all, we show the results for $V_{Si}^-(I,II)$ whose spin multiplicity of quartet has previously been unambiguously determined by ENDOR.¹³

The ENDOR spectrum of $V_{Si}^-(I,II)$ measured at 342.3 mT is shown in Fig. 2(a). At this field, a strong ^{29}Si HF satellite due to 12 next-nearest-neighbor (NNN) Si atoms was observed (see Fig. 1). The ENDOR signals were clearly detected and labeled as ν_{A1} , ν_{A2} , ν_{B1} , ν_{B2} , ν_C , ν_D , and ν_E . The observed frequencies are shown in Table I. Figure 3(a)

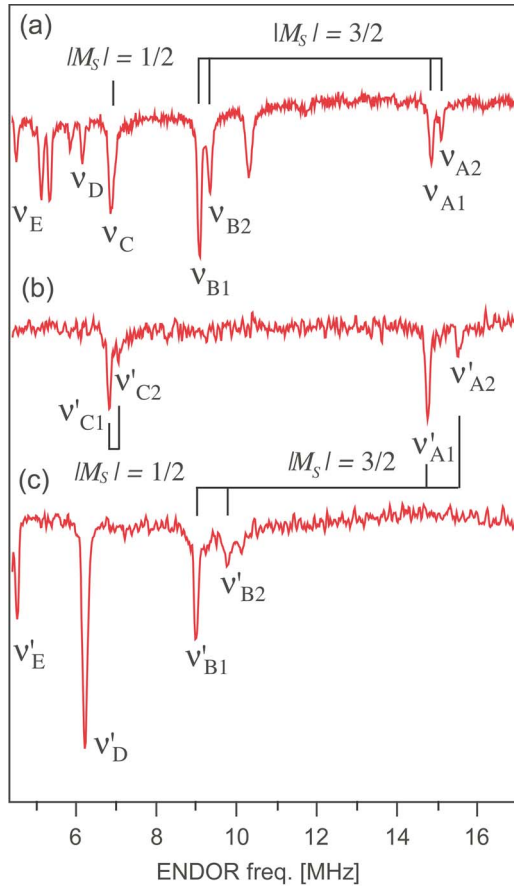


FIG. 2. (Color online) ENDOR spectrum the electron-irradiated *n*-type 4H-SiC at room temperature taken with the magnetic field along the *c* axis ([0001] axis). (a) Spectrum of $V_{Si}^{-}(\text{I,II})$ at 342.3 mT. (b) Spectrum of T_{V2a} at low-field side (339.8 mT). (c) The spectrum of T_{V2a} at high-field side (344.8 mT).

shows the energy-level splitting for a spin quartet ($S=3/2$) state with one nucleus ($I=1/2$), which was calculated using the successive three terms in Eq. (1). As indicated in Figs. 2

TABLE I. Observed and calculated resonant ENDOR frequencies of $V_{Si}^{-}(\text{I,II})$ and T_{V2a} .

		Obs. (MHz)	Calc. (MHz) ^a
$V_{Si}^{-}(\text{I,II})$	ν_{A1}	14.86	14.88
	ν_{A2}	15.11	15.12
	ν_{B1}	9.10	9.09
	ν_{B2}	9.35	9.33
	ν_C	6.89	6.89, 6.97
T_{V2a}	ν'_{A1}	14.76	14.77
	ν'_{A2}	15.53	15.55
	ν'_{B1}	9.00	8.98
	ν'_{B2}	9.79	9.76
	ν'_{C1}	6.83	6.84
	ν'_{C2}	7.06	7.10

^aThe calculated frequencies were derived from Eq. (1) by using the parameters described in the text.

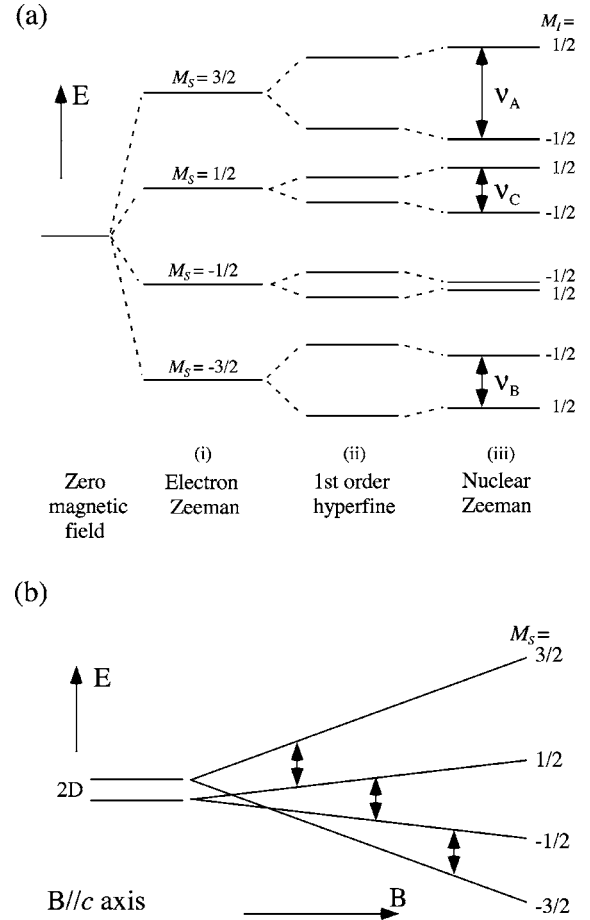


FIG. 3. Energy-level schemes under $A_{\text{eff}} > 0$, $g_n < 0$, and $D > 0$. (a) Energy levels showing the effects of successive terms in Eq. (1) and ENDOR transitions at constant magnetic field. (i) Addition of electron Zeeman interaction. (ii) Addition of the first-order HF interaction. (iii) Addition of nuclear Zeeman interaction. (b) Energy levels with respect to magnetic field and EPR transitions in quartet for $D > 0$ at the $B \parallel c$ axis.

and 3, ν_{A1} , ν_{A2} , ν_{B1} , and ν_{B2} were assigned to the transitions of the $|M_S|=3/2$ manifold, and ν_C was assigned to the transition of the $|M_S|=1/2$ manifold. The present data and analysis are consistent with those reported previously for $V_{Si}^{-}(\text{I,II})$,¹³ except that we could resolve small splittings of about 0.25 MHz between ν_{A1} and ν_{A2} and between ν_{B1} and ν_{B2} . In the previous study, these splittings were not detectable due to a broad linewidth (0.3–0.5 MHz).¹³ Therefore our pulsed ENDOR measurements have higher resolution than those of the previous CW ENDOR studies. We think the origin of these splittings is site splittings for the following reason. We found a signal-intensity ratio of approximately 3:1 for the ν_{A1} and ν_{A2} lines and for the ν_{B1} and ν_{B2} lines. As shown in Fig. 4, the 12 NNN Si atoms are classified into three types: nine basal and three *c*-axial Si atoms according to their locations relative to the NN C atoms. Therefore two split lines with intensity ratio 3:1 are expected for the relevant HF satellite when $B \parallel c$,⁹ which is quite consistent with our observation.²⁶ We calculated the ENDOR frequencies of the transitions of the $|M_S|=3/2$ for $B=342.3$ mT using $A_{\text{eff}}=7.99$ and 8.15 MHz and $g_n=-1.1106$.²⁵ They correspond

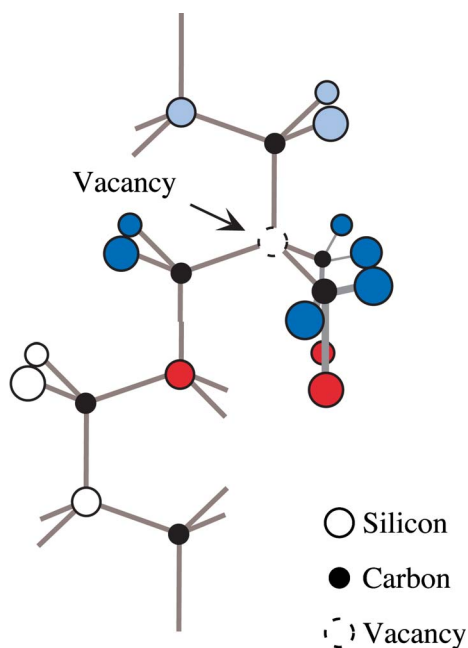


FIG. 4. (Color online) 12 NNN Si atoms of a silicon vacancy. They are classified into three types: nine basal and three c -axial Si atoms according to their locations relative to the NN C atoms. The position of the vacancy is assumed to be hexagonal site in this figure as an example. It should be noted that the number of types is the same as that in the case of the quasicubic site.

well to the measured frequencies of ν_{A1} , ν_{A2} , ν_{B1} , and ν_{B2} as shown in Table I. The parameters of $A_{\text{eff}}=7.99$ and 8.15 MHz are very close to the reported value ($=8.35$ MHz) for the HF coupling constant of the NNN ^{29}Si atoms, which was reported to be isotropic in the EPR measurement.^{9,13} Using the same A_{eff} parameters, we calculated the resonant frequencies for $M_S=1/2$ to be 6.89 and 6.97 MHz. Their difference is only 0.08 MHz, so the site splitting was not resolved for the ν_C line. But looking carefully, we can see that the ν_C line has a small shoulder on the high-frequency side, suggesting the presence of the site splitting. It should be noted that the significant difference in signal intensity of the small splittings excludes the possibility that the small splittings come from the difference in A_{eff} between $V_{Si}(\text{I})$ and $V_{Si}(\text{II})$. In our samples, the concentration of $V_{Si}(\text{I})$ was almost the same as that of $V_{Si}(\text{II})$.⁹ Accordingly, we have consistently reproduced the spin-multiplicity determination for $V_{Si}(\text{I,II})$ even with the much improved resolution. The same procedure is applied to T_{V2a} in the next step. In our measurements, unfortunately, the ENDOR signal of $M_S=-1/2$, whose frequency is estimated to be around 1.1 – 1.2 MHz, could not be identified. It is because the signal intensity at the low-frequency region is very weak due to the instrumental requirement and the spectrum at the low-frequency region is very complicated due to many superpositions of small frequencies of HF interaction at distant sites.

The ENDOR spectra of T_{V2a} measured at 339.8 and 344.8 mT are shown in Figs. 2(b) and 2(c), respectively. We observed signals that can be assigned to the transitions of the $|M_S|=3/2$ manifold. They are labeled ν'_{A1} , ν'_{A2} , ν'_{B1} , and ν'_{B2} , respectively. Likewise in $V_{Si}(\text{I,II})$, the small splittings

were observed. Signals that can be assigned to the transition of the $|M_S|=1/2$ manifold were observed and labeled ν'_{C1} and ν'_{C2} . The observed resonant frequencies and the calculated resonant frequencies are summarized in Table I, where we used $A_{\text{eff}}=7.93$ and 8.45 MHz for the calculation. As shown in Table I, the calculated resonant frequencies correspond well to the observed ones. The A_{eff} parameters of 7.93 and 8.45 MHz correspond to the reported values [8.7 MHz (Ref. 6) and 8.35 MHz (Ref. 12)] for the HF coupling constant of the NNN ^{29}Si atoms, which was reported to be isotropic in the EPR measurement.^{6,12}

Assuming $S=1$, the ENDOR frequencies for $B=339.8$ and 344.8 mT were calculated to be 5.6 ± 0.2 and 11.4 ± 0.2 MHz, respectively, using the reported values of A_{eff} parameters [8.7 MHz (Ref. 6), and 8.35 MHz (Ref. 12)]. As seen from Figs. 2(b) and 2(c), the signal was not observed around these frequencies. Therefore we can conclude that the spin multiplicity of T_{V2a} is not triplet ($S=1$) but must be quartet ($S=3/2$).

It is also notable that the signals labeled ν'_A and ν'_C were observed only in the low-field transition and the signals labeled ν'_B were observed only in the high-field transition, as shown in Figs. 2(b) and 2(c). This can be reasonably explained by the spin- $3/2$ model. The sign of the HF coupling constant of the NNN $^{29}\text{Si}(A_{Si_{\text{NNN}}})$ can be assumed to be positive as reported previously.¹³ On the other hand, the ZFS parameter (D) was reported to be positive from the W -band EPR measurement at 1.2 K.⁷ When $D>0$, the transition of $|S, M_S\rangle=|3/2, 3/2\rangle \leftrightarrow |3/2, 1/2\rangle$ [$|S, M_S\rangle=|3/2, 3/2\rangle \leftrightarrow |3/2, 1/2\rangle$] should be observed on the low-field side, while the transition of $|3/2, -1/2\rangle \leftrightarrow |3/2, -3/2\rangle$ should be observed on the high-field side, as illustrated in Fig. 3(b). Under $A_{\text{eff}}>0$ and $D>0$, it can be derived from Eq. (2) that the signals labeled ν'_A and ν'_C should be observed only in the low-field transition and the signals labeled ν'_B should appear only on the high-field side. These also support our conclusion.

In the ENDOR spectrum of Fig. 2, several signals other than those of the NNN ^{29}Si atoms were observed. We tentatively consider that they are due to HF interactions at distant sites. As for ν_D , ν_E , ν'_D , and ν'_E in Figs. 2(a) and 2(c), they are tentatively assigned as the signals from third NN ^{13}C HF interaction. In the case of ν'_D and ν'_E in Fig. 2(c), assuming that A_{eff} is 1.69 MHz and the sign of it is positive, it is expected to be observed at 4.5 and 6.2 MHz in high-field transition. The frequency of ν'_E is 4.5 MHz and also corresponds to it. By using the value of 1.69 MHz, the other two signals were expected to be observed at 1.2 and 2.8 MHz. However, we could not identify them because the spectrum at the low-frequency region is very complicated due to many superpositions of small frequencies of HF interaction at distant sites. The frequencies of ν_D (6.2 MHz) and ν_E (4.5 MHz) in Fig. 2(a) also correspond to the calculated frequencies of 6.2 and 4.5 MHz by using $A_{\text{eff}}=1.66$ MHz. As for the signal at 10.3 MHz in Fig. 2(a), it may be tentatively assigned to fourth NN Si atoms. Assuming that A_{eff} is 4.94 MHz, the signals at 5.4 and 10.3 MHz are expected to be observed. These correspond well to the signals observed at 5.3 and 10.3 MHz in Fig. 2(a). Probably, other signals are also ENDOR frequencies at distant sites. In the previous study,¹³ these lines were not observed. Maybe this comes

from the different sensitivity of the signals due to the different measurement method with the present study.

Previously, Son *et al.* suggested that T_{V2a} should be a triplet spin state, because its spectrum did not exhibit the central $|S, M_S\rangle = |3/2, 1/2\rangle \leftrightarrow |3/2, -1/2\rangle$ transition in the dark.⁸ In their EPR measurement, however, other signals stronger than the T_{V2a} signal were observed at around the field position where the central transition should appear. It is therefore unclear whether the central transition of a quartet state was really absent or not. As for the measurements under light illumination, Son *et al.* proposed the polarization model with a triplet ground state and a singlet excited state.⁸ On the other hand, we have proposed the model to explain little enhanced $|S, M_S\rangle = |3/2, 1/2\rangle \leftrightarrow |3/2, -1/2\rangle$ transition in any direction of the magnetic field.⁶ Thus their experimental results are still consistent with our conclusion.

Orlinski *et al.* also suggested the spin-1 model for T_{V2a} based on the estimation of the nutation frequency (ω_n) ratios by measuring the pulse lengths needed for the maximum ESE signal.⁷ The estimated ω_n ratios were not consistent with those of our previous nutation experiments,⁶ resulting in the controversy. However, it should be mentioned that those results of ours were obtained from 2D nutation experiments. In principle, the 2D technique gives more accurate and reliable ω_n ratios, especially when the detected ESE signal consists of two or more signals having different ω_n s.^{27,28}

The present conclusion that T_{V2a} should have a quartet spin ($S=3/2$) and should be negatively charged is consistent with the theoretical aspects. The (0/+) and (-/0) levels of the silicon vacancy were predicted to be 0.2–0.3 eV and

0.7–0.8 eV above the valence-band top of 4H-SiC, respectively,¹⁹ which are much lower than the mid gap. Therefore, from the theoretical viewpoint, the silicon vacancy is expected to be negatively charged in our *n*-type SiC. The coexistence of T_{V2a} and $V_{Si}^-(I,II)$ in our samples is quite understandable because they were both negatively charged states of the silicon vacancy. In addition, the spin-3/2 model also explains the high thermal stability of T_{V2a} . According to the first-principles calculation,¹⁹ the formation energy of the silicon vacancy is higher for the neutral charge state than for the negatively charged state, resulting in higher thermal stability for the latter state. This will be related to the fact that the T_{V2a} centers could be present in HPSI SiC even after 1600 °C annealing.¹⁸

IV. SUMMARY

The spin quartet ($S=3/2$) state and the negatively charged (-1) state of T_{V2a} in 4H-SiC have been confirmed by pulsed ENDOR measurements. After demonstrating the spin-multiplicity determination for the known center $V_{Si}^-(I,II)$ ($S=3/2$), we applied the same procedure to the T_{V2a} center. We could observe signals that we assigned to the transitions of the $|M_S|=3/2$ manifold. The observation of the $|M_S|=3/2$ manifold and lack of observation of the transition of the $|M_S|=1$ one at the frequencies expected in the case of $S=1$ clearly indicate that the spin multiplicity of T_{V2a} is quartet ($S=3/2$) and not triplet ($S=1$).

¹E. Janzén, I. G. Ivanov, N. T. Son, B. Magnusson, Z. Zolnai, A. Henry, J. P. Bergman, L. Storasta, and F. Carlsson, *Physica B* **340-342**, 15 (2003).

²V. S. Vainer, V. I. Veigner, V. A. Il'n, and V. F. Tsvetkov, *Sov. Phys. Solid State* **22**, 2011 (1980) [*Fiz. Tverd. Tela* (Leningrad) **22**, 3436 (1980)].

³V. S. Vainer and V. A. Il'n, *Sov. Phys. Solid State* **23**, 2126 (1981) [*Fiz. Tverd. Tela* (Leningrad) **23**, 3659 (1981)].

⁴H. J. von Bardeleben, J. L. Cantin, I. Vickridge, and G. Battistig, *Phys. Rev. B* **62**, 10126 (2000).

⁵E. Sörman, N. T. Son, W. M. Chen, O. Kordina, C. Hallin, and E. Janzén, *Phys. Rev. B* **61**, 2613 (2000).

⁶N. Mizuochi, S. Yamasaki, H. Takizawa, N. Morishita, T. Ohshima, H. Itoh, and J. Isoya, *Phys. Rev. B* **66**, 235202 (2002).

⁷S. B. Orlinski, J. Schmidt, E. N. Mokhov, and P. G. Baranov, *Phys. Rev. B* **67**, 125207 (2003).

⁸N. T. Son, Z. Zolnai, and E. Janzén, *Phys. Rev. B* **68**, 205211 (2003).

⁹N. Mizuochi, S. Yamasaki, H. Takizawa, N. Morishita, T. Ohshima, H. Itoh, and J. Isoya, *Phys. Rev. B* **68**, 165206 (2003).

¹⁰N. Mizuochi, J. Isoya, S. Yamasaki, H. Takizawa, N. Morishita, T. Ohshima, and H. Itoh, *Mater. Sci. Forum* **389-393**, 497 (2002).

¹¹Mt. Wagner, N. Q. Thinh, N. T. Son, P. G. Baranov, E. N. Mokhov, C. Hallin, W. M. Chen, and E. Janzén, *Mater. Sci. Forum* **389-393**, 501 (2002).

¹²M. Wagner, N. Q. Thinh, N. T. Son, W. M. Chen, E. Janzén, P. G.

Baranov, E. N. Mokhov, C. Hallin, and J. L. Lindström, *Phys. Rev. B* **66**, 155214 (2002).

¹³T. Wimbauer, B. K. Meyer, A. Hofstaetter, A. Scharmann, and H. Overhof, *Phys. Rev. B* **56**, 7384 (1997).

¹⁴M. Bockstedte, M. Heid, and O. Pankratov, *Phys. Rev. B* **67**, 193102 (2003).

¹⁵H. Itoh, N. Hayakawa, I. Nashiyama, and E. Sakuma, *J. Appl. Phys.* **66**, 4529 (1989).

¹⁶A. Kawasuso, F. Redmann, R. Krause-Rehberg, T. Frank, M. Weidner, G. Pensl, P. Sperr, and H. Itoh, *J. Appl. Phys.* **90**, 3377 (2001).

¹⁷W. E. Carlos, E. R. Galser, and B. V. Shanabrook, *Mater. Sci. Forum* **457-460**, 461 (2004).

¹⁸N. T. Son, B. Magnusson, Z. Zolnai, A. Ellison, and E. Janzén, *Mater. Sci. Forum* **457-460**, 437 (2004).

¹⁹M. Bockstedte, A. Mattausch, and O. Pankratov, *Phys. Rev. B* **68**, 205201 (2003).

²⁰A. Zywiets, J. Furthmüller, and F. Bechstedt, *Phys. Rev. B* **59**, 15166 (1999).

²¹H. Itoh, M. Yoshikawa, I. Nashiyama, S. Misawa, H. Okumura, and S. Yoshida, *IEEE Trans. Nucl. Sci.* **37**, 1732 (1990); H. Itoh, A. Kawasuso, T. Ohshima, M. Yoshikawa, I. Nashiyama, S. Tanigawa, S. Misawa, H. Okumura, and S. Yoshida, *Phys. Status Solidi A* **162**, 173 (1997).

²²J. Isoya, H. Kanda, Y. Uchida, S. C. Lawson, S. Yamasaki, H. Itoh, and Y. Morita, *Phys. Rev. B* **45**, 1436 (1992).

- ²³T. A. Kennedy and N. D. Wilsey, Phys. Rev. B **23**, 6585 (1981); T. A. Kennedy, N. D. Wilsey, J. J. Krebs, and G. H. Stauss, Phys. Rev. Lett. **50**, 1281 (1983).
- ²⁴J. Hage, J. R. Niklas, and J.-M. Spaeth, Mater. Sci. Forum **10-12**, 259 (1986).
- ²⁵J. A. Weil, J. R. Bolton, and J. E. Wertz, in *Electron Paramagnetic Resonance* (Wiley, New York, 1994).
- ²⁶Strictly, when the magnetic field is parallel to the c axis, two lines with intensity ratio 1:3 are expected in T_d and three lines with intensity ratio 1:2:1 are expected in C_{3v} . We consider that the observation of two lines is due to the small distortion of $V_{Si}^-(I,II)$ from T_d as reported previously (Refs. 6 and 9).
- ²⁷A. Schweiger and G. Jeschke, in *Principles of Pulse Electron Paramagnetic Resonance* (Oxford University Press, Oxford, 2001), Chap. 14, p. 427.
- ²⁸N. Mizuochi, Y. Ohba, and S. Yamauchi, J. Chem. Phys. **111**, 3479 (1999); N. Mizuochi, Y. Ohba, and S. Yamauchi, J. Phys. Chem. A **103**, 7749 (1999).